

Optimizing the phase retardation caused by optical coatings

H. Fabricius*, T. N. Hansen

DELTA Light & Optics, Venlighedsvej 4, DK-2970 Hoersholm, Denmark

ABSTRACT

During the interaction with a coating, a phase shift is introduced on the light. In general this phase shift is different for S and P-polarized light. This means that the state of polarization may be changed during the interaction with the coating. Working with laser beams it is common to polarize the light parallel or orthogonal to the plane of incidence. In this case phase retardation does not occur. This explains why most people forget about the phase performance in their daily work. On the other hand, it is possible to utilize the phase retardation. For example it is possible to design a coating transforming a linearly polarized beam into a circularly polarized beam, and it is possible to make the phase retardation independent of the wavelength in a certain wavelength range. Equations and a design technique are presented for first and second order optimization of the phase retardation on reflection or transmission of light from optical coatings. The optimization is performed by alternating optimization on the phase characteristics and the phase targets for S and P-polarized light. Examples of the design of laser mirrors with zero retardation and quarter wave retardation are presented.

Keywords: phase retardation, second order optimization, co-optimization, quarter-wave, half-wave

1. INTRODUCTION

The main subject of this paper is the design of phase retarding optical coatings. This is a theoretical matter. However, to make this text more appealing to you, we have decided to introduce three practical examples of optical systems, where this kind of coating could be used.

One obvious example is the laser mirror with zero phase retardation. This kind of mirror manages to reflect collected light with a un-known state of polarization, without altering it. This is important in some sensor systems and in some medical systems. The mirror easily handles both out-going and in-going light.

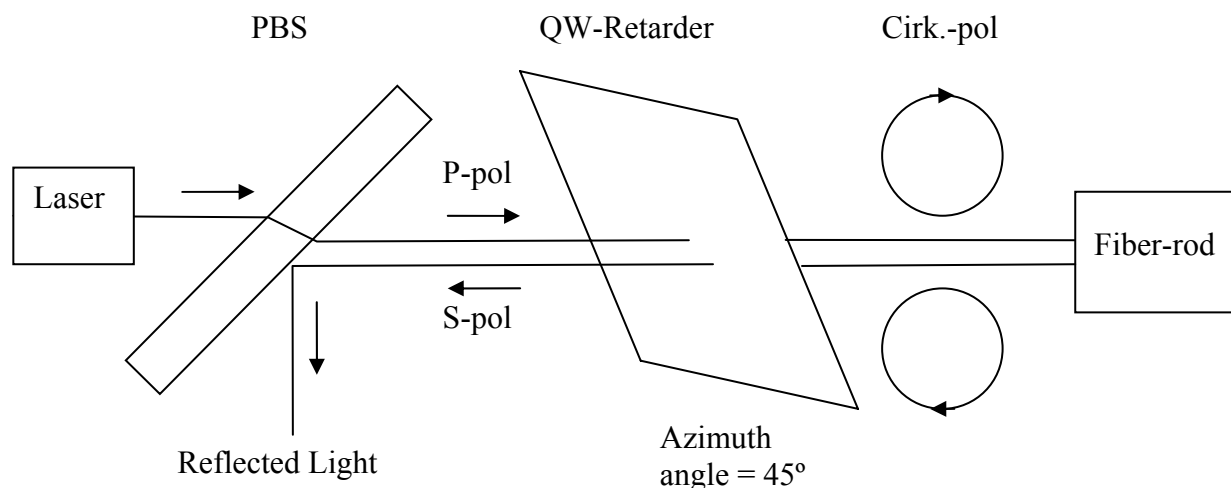


Fig. 1. Schematic drawing of a dental laser system with two thin-film components suppressing reflected laser light from an un-coated and replaceable fiber rod

* hff@delta.dk; phone +45 7219 4724; fax +45 7219 4001; www.delta.dk

Another obvious example is the Quarter-Wave retarder. It is used to convert linearly polarized laser light into circularly polarized laser light. Figure 1 shows an example where a polarizing beam-splitter on a plate and a quarter-wave retarding filter with nearly no reflection is used to suppress the back-reflection from an un-coated and replaceable glass rod in the front of a dental laser. It is easier to design a quarter wave retarding mirror than to design a quarter wave retarding and highly transmitting filter. However, the advantage of the later is that it only offsets the optical beam path slightly, although the angle of incidence (AOI) as well as the azimuth angle is 45° .

A more complex but important example is shown in figure 2.

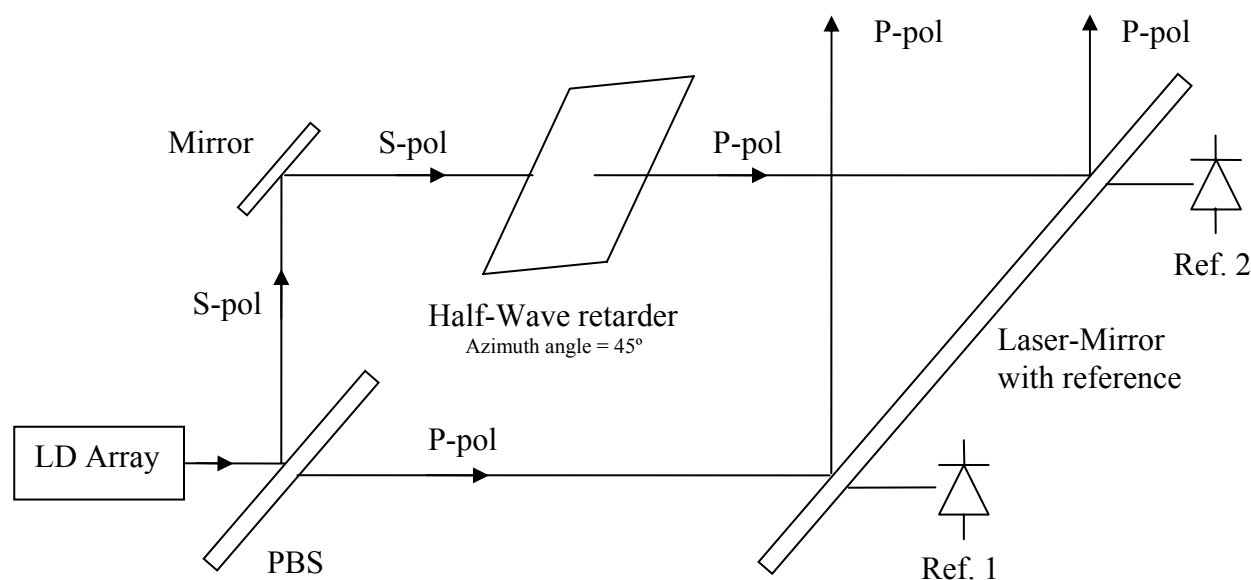


Fig. 2. Schematic drawing of a power monitoring system for a high power laser diode array used in a medical device. The laser light entering the system is random polarized. The laser mirror seen at the right transmits a small amount of the P-polarized light, whereas “all” of the S-polarized light is reflected. A wideband polarizing beam-splitter on a blank is used to separate the S-polarized light. A thin-film half wave retarder is used to convert the S-polarized light into P-polarized light. This enables a monitoring of the total power in the laser beam. The fact that the laser light is split into two beams is not a problem in the actual system.

A high power laser diode array is used for a medical laser system. Each laser-diode in the array couples the laser light into an optical fibre. At the other end of the fibres, the light is collimated with optical lenses. In order to monitor the laser power, the laser light is reflected by a laser mirror with a small reference take out (we call it a laser mirror with reference). Figure 4 shows an example of the transmission of such a laser mirror for 45° degrees of incidence. It is important that the transmission is independent of the laser wavelength in a certain wavelength range. Typical tolerances on the wavelength of the laser light could be $\pm 20\text{nm}$. It is not realistic to design a laser mirror with equal transmission of S and P-polarized light. In this case we did design a mirror transmitting a small and constant amount of P-polarized light and reflecting “all” of the S-polarized light.

Unfortunately the state of polarization of the total laser beam arriving from the fibre bundle is quite unstable. Of this reason, it is important to monitor the power of the sum of the S and the P-polarized light. In order to do this we introduce a couple of thin-film components.

The first component is a special kind of polarizing beam-splitter developed by DELTA back in 2000^{1,2}. It is a polarizing beam splitter on a blank – which makes it stand high power. However, in contrast to the classical LP type, this combined LP and SP type works in a wavelength range fitting the tolerances on the laser wavelength of the laser diode array (see

figure 3a and 3b). It is like a polarizing band pas filter for 45 degrees of incidence, working as a polarizing beam-splitter in a wavelength range 60nms wide. It was displayed in action for a different wavelength at the DELTA stand at the Laser 2001 exhibition in Munich. This type of polarizing beam-splitter is used with great success in different types of medical laser systems at present.

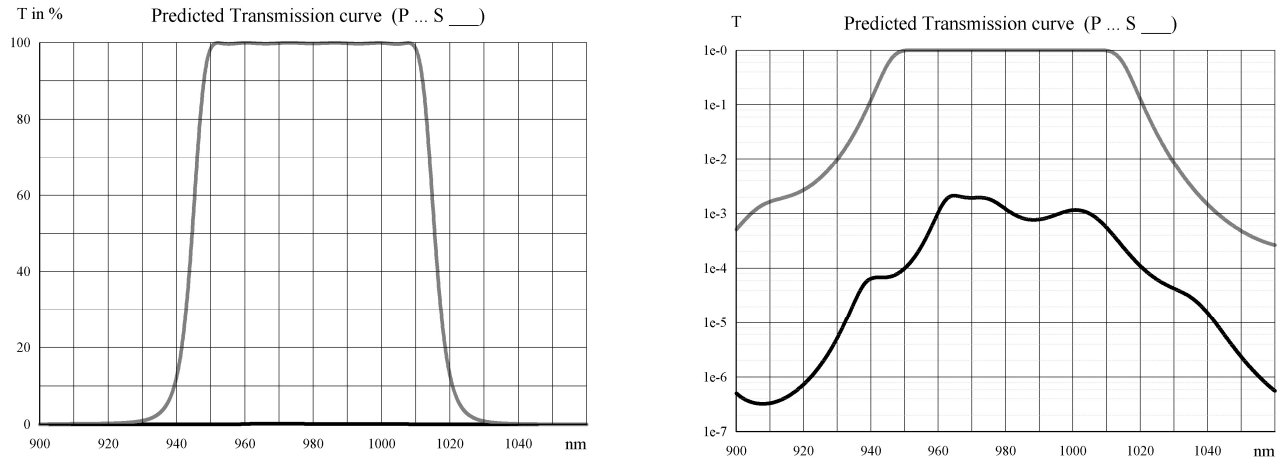


Fig. 3. Figure at the left shows the predicted transmission of S-polarized and P-polarized light for a polarizing beam-splitter produced on a blank. The figure at the right shows the corresponding curves in logarithmic scale. The polarization splitting is efficient in a wavelength range 60nms wide whereas the applied laser diode array in figure 2 requires a working range of 980nm +/- 20nms. That is an extraordinary performance of a PBS on a blank. The fact that the PBS is unglued makes it stand a lot of power, and it is for sure suited for mass production. S-polarized light is suppressed by a factor of 500.

The second component is a standard laser mirror. The last component is a thin-film half wave retarder. It is designed to be placed at an angle of incidence (AOI) of 45 degrees. At an azimuth angle of 45 degrees, the half wave retarder³ switches the S-polarized light into P-polarized light. It is possible to tune the phase retardation by altering the azimuth angle³. In the following we will see how to design this thin-film component. DELTA Light & Optics manage to produce the coatings mentioned in the shape of Ultra Hard surface coatings suited for production in amounts and for cutting into custom specified dimensions.

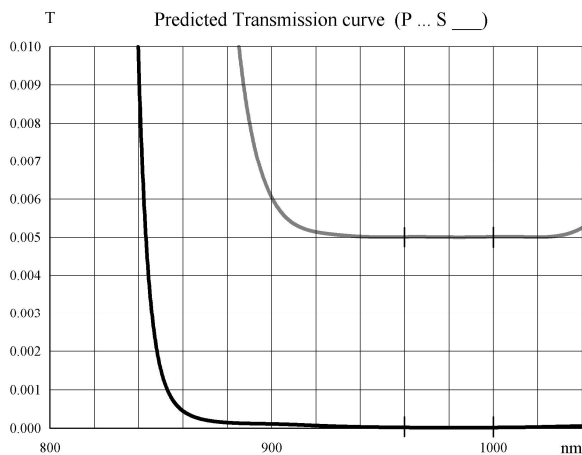


Fig. 4. Predicted transmission of S and P-polarized light for a laser-mirror with reference. AOI is 45 degrees. The laser mirror transmits a visible guidance light at 635nm. The transmission of P-polarized light is independent of the wavelength from 940nm to 1020nm. S-polarized light is practically fully reflected.

2. THE MERIT FUNCTION

The basis of all computer-based optimizations is a stepwise reduction of the deviation between a certain target and the estimated performance of a construction^{1,2,4-6}. A single number describing the deviation is calculated with a merit function. It is common to apply equation 1 for the optimization of a single property, u , at a fixed angle of incidence and S or P-polarized light

$$F_u = \sum_{k=1}^L v(u_k) \cdot [u_k - \bar{u}_k]^{2p} \quad p \in Z_+ \quad (1)$$

u in example could be the reflection, transmission or phase shifts introduced by the coating at the L sampling points and \bar{u} the corresponding desired target values. $v(u_k)$ is the spectral weighting of the sampling at λ_k . The merit function simply is the least square deviation between the desired and the obtained characteristics, when p is equal to one. The sensitivity towards large deviations may be increased by application of a larger exponent $2p$ where p is a positive integer.

The dependence on the state of polarization in general is taken into account by introduction of the following main expression¹

$$F = \sum_{a=1}^M b_a \cdot [c_s \cdot F_{s-pol}(\theta_a) + c_p \cdot F_{p-pol}(\theta_a)] \quad (2)$$

where c_s is the relative weighting of the s-polarized light, c_p the relative weighting of the p-polarized light and b_a the weighting of the angle segment indexed a .

In order to enable the co-optimization of several parameters we introduce the following expression¹ describing the contributors for equation 2

$$F_{x-pol}(\theta_a) = \sum_{m=1}^N c_m \cdot F_{m,x-pol}(\theta_a) \quad (3)$$

where c_m is the weighting of the contributor m and where x symbolises s or p. According to equations 2 and 3 the merit function is composed of a number of additive contributions F_m and the first and second derivatives in respect to changes in the layer thicknesses do not cross link. This means that we may discuss the calculation of each of the contributors F_m separately. In the following we will try to co-optimize the reflection or transmission and the associated phase shifts for different ultra hard surface coatings.

3. SECOND ORDER OPTIMIZATION (NEWTON TYPE)

The most common and widely used technique for optimization of optical multi-layers is the first order optimization technique (e.g. steepest descent method or the simplex method^{1,5}). Unfortunately those techniques are very slow in practice^{1,2,5,6}. In order to use the needle synthesis technique⁴ for the design of the desired kind of coatings, it is important to have the ability to fully optimize a coating with a certain number of layers. In order to do this efficiently second order optimization for sure is needed and it must be analytically based.

Performing a matrix-inversion on the Hesse matrix, it is possible to make a direct estimate of the optimal layer-code \vec{x}_1 as expressed by

$$\left. \frac{\partial F}{\partial \vec{x}} \right|_{\vec{x}_0} = \overline{\overline{H}} \cdot (\vec{x}_0 - \vec{x}_1) \quad \Rightarrow \quad \vec{x}_1 = \vec{x}_0 - \overline{\overline{H}}_{\vec{x}_0}^{-1} \left. \frac{\partial F}{\partial \vec{x}} \right|_{\vec{x}_0} \quad (4)$$

In practice it is recommendable to try to reach the solution at \vec{x}_1 in more than just a single step⁷ as expressed by

$$\vec{x}_2 = \vec{x}_0 - (1 - c_x) \cdot \overset{=-1}{H}_{\vec{x}_0} \frac{\partial F}{\partial \vec{x}} \Big|_{\vec{x}_0} \quad \text{where } c_x < 1 \quad (5)$$

where $\overset{=-1}{H}_{\vec{x}_0}$ symbolizes the inverted two dimensional Hesse matrix. The elements in the two dimensional complex matrix are described by

$$\frac{\partial^2 F}{\partial d_i \partial d_j} = \sum_{a=1}^M b_a \sum_{m=1}^N c_m \cdot \frac{\partial^2 F_m(\theta_a)}{\partial d_i \partial d_j} \quad (6)$$

where b_a is the weighting of the different angular sections in case of non-collimated light and where c_m is the weighting of the different properties selected for optimization, e.g. the reflection and the phase-retardation.

In our in house developed design software, the merit value is calculated at five different values of c_x (0, 0.2, 0.4, 0.6, 0.8) and a golden section search⁸ and a final parabolic fit is used to determine the optimal value of c_x .

Sometimes the extreme point located by the calculations is a maximum instead of a minimum. In this case it is necessary to step in the opposite direction, and use small steps initially as used for the first order optimization technique.

Second order optimization of optical coatings is much more efficient and much quicker than first order optimization. This is especially the case when the number of layers is large and when close to the final solution.

4. CALCULATION OF THE DERIVATIVES

In most cases it is possible to write the contributions to the merit function on the form shown in equation 1¹. This is for example true for the transmission and reflection of light in the forward and backward directions and the corresponding phase shifts.

Performing a first order optimization or a needle scan we need to calculate the first order derivative of F_u

$$\frac{\partial F_u}{\partial d_j} = \sum_{k=1}^L v(u_k) \cdot 2p \cdot [u_k - \bar{u}_k]^{2p-1} \cdot \frac{\partial u_k}{\partial d_j} \quad (7)$$

To perform a second order optimization we also need to calculate the second order derivative

$$\frac{\partial^2 F_u}{\partial d_i \partial d_j} = \sum_{k=1}^L v(u_k) \cdot 2p \cdot (2p-1) \cdot [u_k - \bar{u}_k]^{2p-2} \cdot \frac{\partial u_k}{\partial d_i} \cdot \frac{\partial u_k}{\partial d_j} + \sum_{k=1}^L v(u_k) \cdot 2p \cdot [u_k - \bar{u}_k]^{2p-1} \cdot \frac{\partial^2 u_k}{\partial d_i \partial d_j} \quad (8)$$

The calculation of the first and the second order derivatives of u_k is not a simple task as u_k is a function of the matrix-product of as many complex matrices as layers in the coating. The calculation of u_k and the derivatives was shown in detail in a larger report¹ from DELTA. However in this text we will limit ourselves to discuss the subject at a higher level.

5. CALCULATION OF THE PHASE SHIFTS

The amplitude transmission and reflection coefficients are complex quantities, and we may write them on the polar form

$$r = \rho \cdot \exp(i\phi_r) \quad (9)$$

$$t = \tau \cdot \exp(i\phi_t) \quad (10)$$

where the quantities ϕ_r and ϕ_t symbolizes the phase shifts resulting from the reflection and transmission of light in the boundary between the two media. Similar expressions exist for the reflection and transmission in reverse direction. Writing the amplitude reflection or transmission coefficient as

$$\tilde{w}_k = w_{k1} - i \cdot w_{k2} \in [t, r, t_r, r_r] \quad (11)$$

where the index r refers to the reverse direction, it is possible to calculate the associated phase shift by

$$u_k = \tan^{-1}\left(\frac{-w_{k2}}{w_{k1}}\right) + p_k \cdot 2\pi \quad (12)$$

where p_k is an integer and k the index of the sampling points. In a vector plot, u_k is a vector in the complex plan. This means that we have to add π to the result of a computer calculation of the \tan^{-1} when the vector is inside the second or the third quadrant, and 2π if the vector is in the fourth quadrant. The optimal values of p_k are found by checking the characteristic for 2π discontinuities.

6. OPTIMIZATION OF THE PHASE-PERFORMANCE

We need to calculate the first and second order derivatives of u in respect to the thickness of the layers d_j . The first derivative is obtained by differentiation of equation 12

$$\frac{\partial u_k}{\partial d_j} = \left[1 + \left(\frac{-w_{k2}}{w_{k1}} \right)^2 \right]^{-1} \cdot \frac{\partial}{\partial d_j} \left(\frac{-w_{k2}}{w_{k1}} \right) = \left[w_{k1}^2 + w_{k2}^2 \right]^{-1} \cdot \left[w_{k2} \cdot \frac{\partial w_{k1}}{\partial d_j} - w_{k1} \cdot \frac{\partial w_{k2}}{\partial d_j} \right] \quad (13)$$

The second order derivative is found by differentiation of equation 13

$$\begin{aligned} \frac{\partial^2 u_k}{\partial d_i \partial d_j} = & -2 \cdot \frac{\partial u_k}{\partial d_j} \cdot \left[w_{k1}^2 + w_{k2}^2 \right]^{-1} \cdot \left[w_{k1} \cdot \frac{\partial w_{k1}}{\partial d_i} + w_{k2} \cdot \frac{\partial w_{k2}}{\partial d_i} \right] \\ & + \left[w_{k1}^2 + w_{k2}^2 \right]^{-1} \cdot \left[\frac{\partial w_{k2}}{\partial d_i} \cdot \frac{\partial w_{k1}}{\partial d_j} - \frac{\partial w_{k1}}{\partial d_i} \cdot \frac{\partial w_{k2}}{\partial d_j} + w_{k2} \cdot \frac{\partial^2 w_{k1}}{\partial d_i \partial d_j} - w_{k1} \cdot \frac{\partial^2 w_{k2}}{\partial d_i \partial d_j} \right] \end{aligned} \quad (14)$$

7. ALTERNATING OPTIMIZATION OF THE PHASE RETARDATION AND THE TARGET

Optimizing the phase-retardation introduced by a coating, the shape of $\bar{u}(\lambda_k)$ may be unimportant. In this case we will introduce the following modular phase-targets

$$\bar{u}_s(\lambda_k) = B / \lambda_k + A \quad (15)$$

$$\bar{u}_p(\lambda_k) = B / \lambda_k + A + C_R \quad (16)$$

Limiting ourselves to the application of a fixed exponent of two in the phase contribution to the merit-function, it may be written as

$$F_u = c_s \sum_{a=1}^M b_a \sum_{k=1}^L v(u_k) \cdot [u_s(\lambda_k) - B/\lambda_k - A]^2 + c_p \sum_{a=1}^M b_a \sum_{k=1}^L v(u_k) \cdot [u_p(\lambda_k) - B/\lambda_k - A - C_R]^2 \quad (17)$$

Where b_a represents the weighting of the contributions from the M angle segments, and where c_s and c_p represents the weighting of s and p -polarized light.

The optimal values of the coefficients A and B must fulfil the following requirements

$$\begin{aligned} \frac{\partial F_u}{\partial A} = c_s \sum_{a=1}^M b_a \sum_{k=1}^L -2 \cdot v(u_k) \cdot [u_s(\lambda_k) - B/\lambda_k - A] \\ + c_p \sum_{a=1}^M b_a \sum_{k=1}^L -2 \cdot v(u_k) \cdot [u_p(\lambda_k) - B/\lambda_k - A - C_R] = 0 \end{aligned} \quad (18)$$

and

$$\begin{aligned} \frac{\partial F_u}{\partial B} = c_s \sum_{a=1}^M b_a \sum_{k=1}^L -2 \cdot v(u_k) \cdot (1/\lambda_k) \cdot [u_s(\lambda_k) - B/\lambda_k - A] \\ + c_p \sum_{a=1}^M b_a \sum_{k=1}^L -2 \cdot v(u_k) \cdot (1/\lambda_k) \cdot [u_p(\lambda_k) - B/\lambda_k - A - C_R] = 0 \end{aligned} \quad (19)$$

Hence, A and B are found by calculation of

$$A = \frac{S_3 \cdot S_5 - S_2 \cdot S_6}{S_1 \cdot S_5 - S_2 \cdot S_6} \quad B = \frac{S_1 \cdot S_6 - S_3 \cdot S_4}{S_1 \cdot S_5 - S_2 \cdot S_6} \quad (20)$$

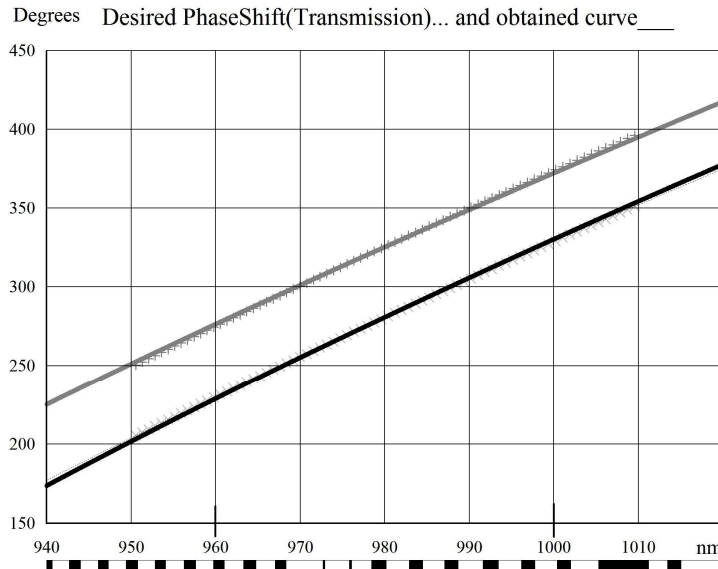
where

$$\begin{aligned} S_1 &= \sum_{a=1}^M b_a \cdot \sum_{k=1}^L v(u_k) & S_2 = S_4 &= \sum_{a=1}^M b_a \cdot \sum_{k=1}^L v(u_k) / \lambda_k \\ S_3 &= \sum_{a=1}^M b_a \cdot \sum_{k=1}^L v(u_k) \cdot [c_s \cdot u_s(\lambda_k) + c_p \cdot u_p(\lambda_k) - c_p \cdot C_R] & S_5 &= \sum_{a=1}^M b_a \cdot \sum_{k=1}^L v(u_k) / \lambda_k^2 \\ S_6 &= \sum_{a=1}^M b_a \cdot \sum_{k=1}^L v(u_k) \cdot [c_s \cdot u_s(\lambda_k) + c_p \cdot u_p(\lambda_k) - c_p \cdot C_R] / \lambda_k \end{aligned} \quad (21)$$

The first part of the optimization of the phase characteristics is obtained performing an alternating optimization on the phase characteristics and the modular phase targets. However, it is recommended to fix the target curves as soon as they stabilize.

8. DESIGNING A TRANSMITTING QUARTER WAVE RETARDING FILTER

In order to design a phase retarding filter, it is necessary to tilt it and to launch equally amounts of S and P-polarized light into it. In the following we use an AOI of 45° and an azimuth angle of 45° to accomplish this (please see figure 1). A transmitting filter only offsets the optical axis slightly doing so. This is clearly of advantage as compared to a phase retarding mirror. On the other hand the light passes two coated surfaces, and the reflection losses need to be as low as possible. In order to make a QW-retardation³ each coating must introduce a phase-retardation half of that.



The desired coating was designed by means of the needle synthesis technique and second order optimization as described in this paper. The applied merit-function was

$$F = F_T + 0.0253 \cdot F_{\phi_i} \quad (22)$$

And the applied phase retardation was $C_R = \pi/4$.

Fig. 5. Screen shot from the design software. Structure at the bottom is the layer structure designed (black is TiO_2 and white is SiO_2). Black solid curve is the phase shift on transmission of S-polarized light. Gray solid curve is the phase shift of P-polarized light. The desired phase retardation is 45°.

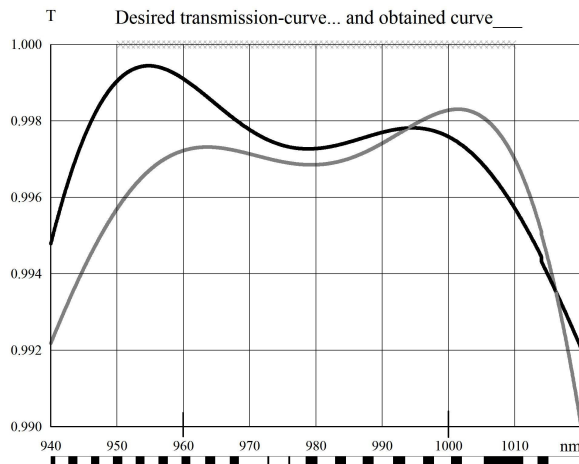


Fig.6. Predicted transmission of S and P-polarized light.

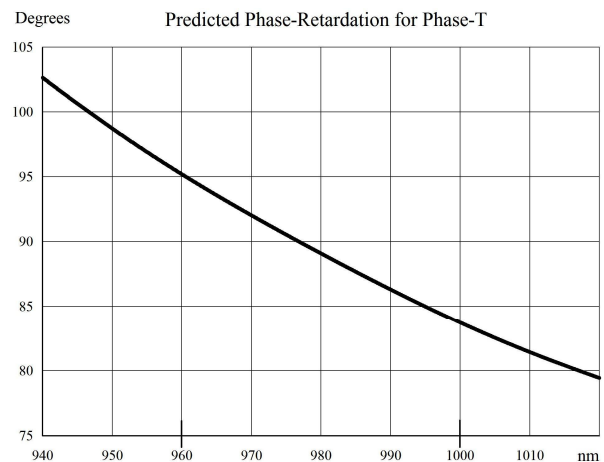


Fig. 7. Predicted total phase retardation of the QW-retarder.

9. DESIGNING A TRANSMITTING HALF-WAVE RETARDER

A half-wave retarder³ is needed to convert the S-polarized light into P-polarized light in the system shown in figure 2. In order to make a highly transmitting HW-retarder each of the coatings must introduce a QW-retardation. Hence C_R in equation 16 is $\pi/2$. Figure 8 shows the predicted phase shifts of S and P-polarized light as function of the wavelength as seen at the end of the needle synthesis of the desired coating.

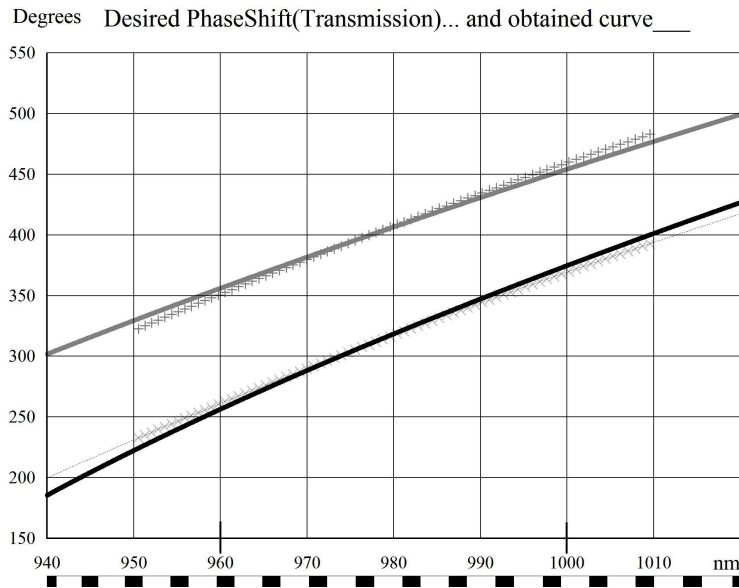
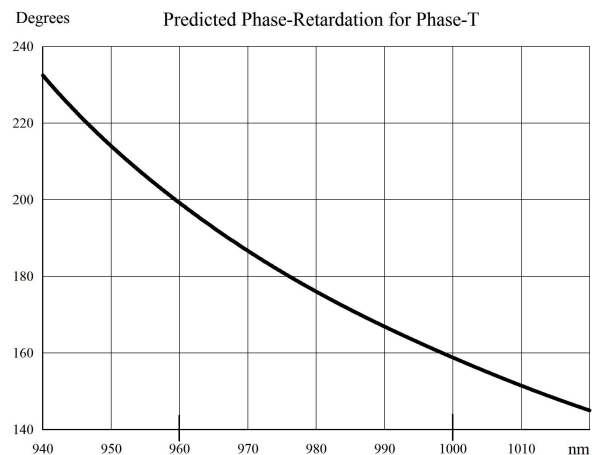
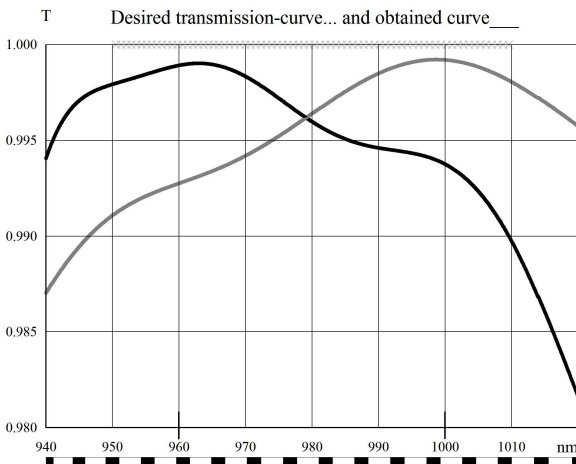


Fig. 8. Figure shows the predicted phase shifts of S and P-polarized light as function of the wavelength as seen at the end of the needle synthesis of the desired coating. The signs + and x marks the entered target points. By comparison with figures 5 & 7 it is seen, that the half wave retarder performs less optimal than two quarter wave retarders in series.



Figures 9 & 10. Figure at the left shows the predicted transmission of S and P-polarized light through the designed half-wave retarder. Although the reflection is low – it is not necessarily lower than the total reflection of two of the designed QW-retarders in series. Figure at the right shows the predicted total phase retardation of the half wave retarder as function of the wavelength. At least 97% of the S-polarized light is converted into P-polarized light in the specified wavelength range. Although it is not perfect it is still quite good.

10. EVALUATED SYSTEM PERFORMANCE

The direction of rotation of the elliptically polarized light in figure 1 changes as the laser light is reflected by the uncoated fiber rod. When the laser light passes the QW-retarder the second time the phase retardation added by the first pass is added once more. This means that in both systems the fraction of light, Y , converted from S-polarization to P-polarization or from P-polarization to S-polarization is given by

$$Y = \frac{1}{2} - \frac{1}{2} \cdot \cos(\phi_t) \quad (23)$$

where ϕ_t is the total phase retardation introduced passing the phase retarding section. The equation was derived by application of Jones matrices³. Figure 11 shows a graphical plot of the relation between Y and ϕ_t .

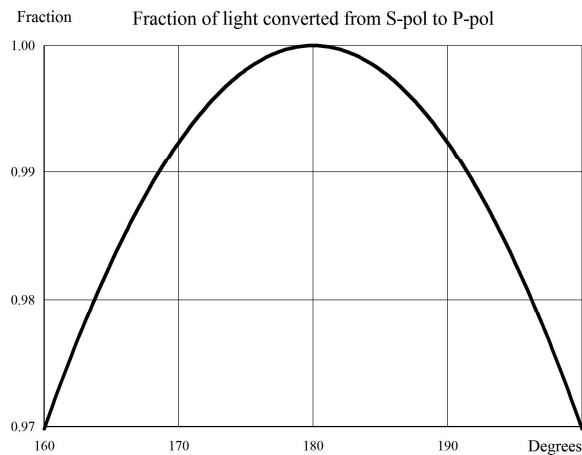


Fig. 11. Figure at the left shows the converted fraction of S-polarized light as function of the total phase retardation in degrees.

By combining the information in figures 7, 10 and 11 it is possible to evaluate the predicted performance of the proposed systems on insertion of the developed phase retarders. Table 1 summarizes the results.

System	Retarders	Wavelength range	Predicted performance
Laser isolator (fig. 1)	QW-retarder (fig. 7)	960 – 1000nm	Rejection > 100
Power monitor (fig. 2)	2 * QW-retarder (fig. 7)	960 – 1000nm	Converted fraction > 99%
Power monitor (fig. 2)	HW-retarder (fig. 10)	960 – 1000nm	Converted fraction > 97%

Table 1. Predicted performance of the proposed thin-film solutions shown in figures 1 and 2 on insertion of the phase retarders designed in sections 8 and 9.

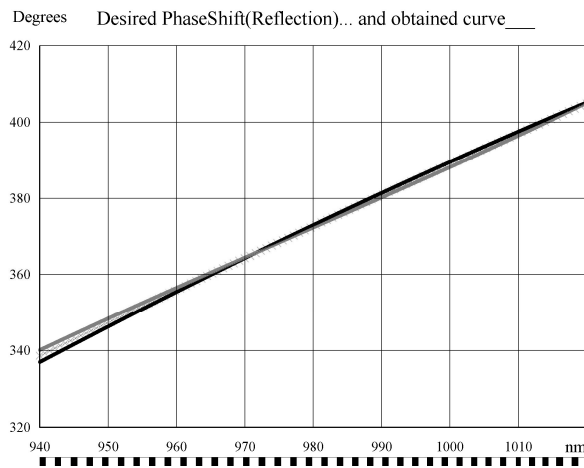
DELTA has produced laser isolators consisting of polarizing beam-splitter cubes and crystalline phase retarders for more than 15 years. The predicted performance of the proposed alternative solution competes well with the existing one in respect to blocking of the reflected laser light.

Two QW-retarders in series converts a larger fraction of S-polarized light into P-polarized light in the power monitoring system. However the >97% obtained by inserting the half wave retarder is still quite good. Assuming that approximately half of the laser light from the high power laser diode array is P-polarized, the power monitor would monitor at least 98.5% of the emitted power.

11. DESIGNING A LASER MIRROR WITH MINIMAL PHASE RETARDATION

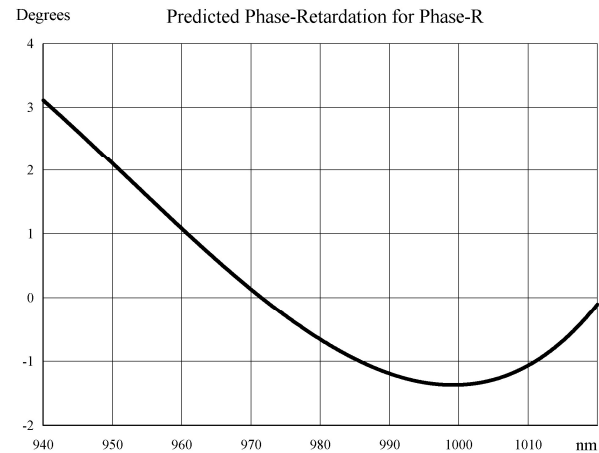
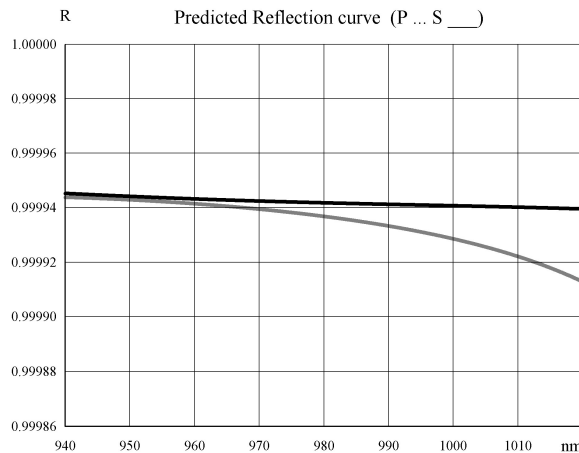
Designing a laser mirror with minimal phase retardation on reflection is also a possibility. In this case the applied merit function is

$$F = F_R + 0.0253 \cdot F_{\phi_r} \quad (24)$$



Figures 12 to 14 show the predicted performance of the laser mirror. The predicted reflection is very high and the phase retardation on reflection is only 1 – 2 degrees. The number of layers is 72 and the coating consists of TiO₂ and SiO₂.

Fig. 12. Figure shows the predicted phase shifts on reflection of S and P-polarized light from the mirror designed. Structure at the bottom is the layer structure designed (black is TiO₂ and white is SiO₂). Figure 14 shows the corresponding predicted phase retardation on reflection.



Figures 13 & 14. Figure at the left shows the predicted reflection of S and P-polarized light from the mirror designed. Figure at the right shows the predicted phase retardation on reflection. It is only 1 – 2 degrees in the desired wavelength range.

12. CONCLUSIONS

A structured merit-function was introduced, which enables a co-optimization of the different properties of an optical coating. Equations were presented, enabling an efficient first and second order optimization of the phase shifts introduced by optical coatings on transmission and reflection of light. Techniques for the alternating optimization of the spectral curves and the phase targets were introduced and applied on different coating designs. A quarter-wave retarding thin-film component with high transmission was designed. A similar half wave retarding component was presented and the performance was compared with that of two QW-retarders. Finally a laser mirror with minimal phase retardation on reflection was designed. It was shown how to use the QW-retarder to suppress back reflection of laser light in a medical laser system with a high power laser diode and how to use a half wave retarder to improve the monitoring of the total laser power in a medical laser system pumped by a high power laser diode array.

REFERENCES

- [1] Henrik Fabricius, *Design and Production of Ultra-hard Optical Thin-films*, DELTA proprietary report, 190 pages, language English (December 2000).
- [2] Henrik Fabricius, "Synthesis and functioning of SMART-coatings for application in compact instruments and sensors," DOPS-NYT 1-2001, p.28-38, The quarterly journal of the Danish Optical Society, 2001
- [3] Amnon Yariv, *Optical Waves in Crystals*, Chapter 5, 1984 by John Wiley & Sons, Inc. ISBN 0-471-09142-1
- [4] Sh. A. Furman and A. V. Tikhonravov, *Basics of Optics of Multilayer Systems*, Chapter 1, Editions Frontieres, France, 1992, ISBN 2-86332-110-2
- [5] Heather M. Liddell, *Computer-aided Techniques for the Design of Multilayer Filters*, Published by Adam Hilger Ltd. Bristol, 1981.
- [6] Alexander Tikhonravov, Michael Trubetskov, "Thin film coatings design using second order optimization methods," Thin Films for Optical Systems, SPIE Proceedings Vol. 1782, pp. 156-164 (1992).
- [7] D. E. Kirk, *Optimal Control Theory – An Introduction*, pp. 344-347, Network Series, Prentice-Hall Inc. 1970
- [8] C. Holm, "Optical thin film production with continuous reoptimization of layer thicknesses", Applied Optics, Vol. 18, p. 1978 – 1982 (1979)